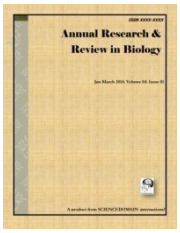

Annual Research & Review in Biology
4(19): 2938-2956, 2014

SCIENCEDOMAIN *international*
www.sciencedomain.org

Performance Analysis of Denoising in MR Images with Double Density Dual Tree Complex Wavelets, Curvelets and Non-subsampled Contourlet Transforms

V. Krishnakumar[1*] and Latha Parthiban[1]

[1]*Department of CSE, Pondicherry University, Puducherry, India.*

Authors' contributions

This work was carried out in collaboration between both authors. Author VK is the major author. He designed the study, performed the analysis, and also drafted the manuscript. Author LP analyzed the results and provided helpful comments. Both authors read and approved the final manuscript.

Original Research Article

Received 22nd January 2014
Accepted 29th March 2014
Published 20th May 2014

ABSTRACT

Digital images are extensively used by the medical doctors during different stages of disease diagnosis and treatment process. In the medical field, noise occurs in an image during two phases: acquisition and transmission. During the acquisition phase, noise is induced into an image, due to manufacturing defects, improper functioning of internal components, minute component failures and manual handling errors of the electronic scanning devices such as PECT/SPECT, MRI/CT scanners. Nowadays, healthcare organizations are beginning to consider cloud computing solutions for managing and sharing huge volume of medical data. This leads to the possibility of transmitting different types of medical data including CT, MR images, patient details and much more information through internet. Due to the presence of noise in the transmission channel, some unwanted signals are added to the transmitted medical data. Image denoising algorithms are employed to reduce the unwanted modifications of the pixels in an image. In this paper, the performance of denoising methods with two dimensional transformations of nonsubsampled contourlets (NSCT), curvelets, double density dual tree complex wavelets (DD-DTCWT) are compared and analysed using the image quality measures such as peak signal to noise ratio, root mean square error, structural similarity index. In

**Corresponding author: Email: vkichu77@gmail.com;*

this paper, 200 MR images of brain (3T MRI scan), heart and breast are selected for testing the noise reduction techniques with above transformations. The results shows that the NSCT gives good PSNR values for random and impulse noises. DD-DTCWT has good noise suppressing capability for speckle and Rician noises. Both NSCT and DD-DTCWT copes well in images affected by poisson noises. The best PSNR value obtained for salt and pepper and additive white Guassian noises are 21.29 and 56.45 respectively. For speckle noises, DD-DTCWT gives 33.46 and it is better than NSCT and curvelet. The values 33.50 and 33.56 are the top PSNRs of NSCT and DD-DTCWT for poisson noises.

Keywords: Nonsubsampled contourlet; curvelet; double density dual tree complex wavelets; denoising, noise removal, medical image processing.

1. INTRODUCTION

Magnetic Resonance Imaging technique is universally used to obtain detailed visual information about the internal organs of the body. The main advantage of MRI is its ability to show higher contrast between the soft tissues of the body than computed tomography (CT). So it is widely used in obtaining neurological (brain), gastrointestinal, musculoskeletal, cardiovascular, and ontological (cancer) images. MRI uses a powerful magnetic field to align the nuclear magnetization of (usually) hydrogen atoms in water in the body. The orientation of the magnetization is adjusted by the radio frequency (RF) waves to produce a rotating magnetic field that are recognized by the scanner, i.e. the resonance frequency of the magnetic field produced by the RF transmitter is used to flip the photons. After the field is turned off, the protons settles to its original spin-down state and the difference in energy between the two states is released as a photon. An image can be constructed because the photons in different tissues return to their equilibrium state at different rates. By changing the parameters on the scanner this effect is used to create contrast between different types of body tissue. The photons returns to its equilibrium state by the independent processes of T1 and T2 relaxation. T1 relaxation is characterized by the longitudinal return of the net magnetization to its ground state in the direction of the main magnetic field. This occurs when spins in the high and low energy state exchange with loss of energy to the surrounding lattice. T2 relaxation occurs when spins in the high and low energy state exchange without losing energy to the surrounding lattice.

The raw data generated by the scanner is complex in nature and is corrupted with zero mean Gaussian distributed noise. After applying inverse Fourier transformation, the resulting real and imaginary data are still Gaussian distributed due to the orthogonality and linearity property of the Fourier transform. MR magnitude images are obtained by taking the square-root of the sum of the square of the real and imaginary images pixel by pixel. After this nonlinear transformation, MR magnitude data can be shown to be Rician distributed.

Medical Imaging is a popular technique applied in the medical field where the internal organs can be viewed without incursion of human body. Medical image processing comprises of several important tasks such as noise suppression, registration [1], segmentation [2], reconstruction [3] and compression [4]. Over the years, various effective algorithms are formulated to solve the medical imaging problems. Noise occurs in CT/MR images during two phases: Acquisition and transmission. During the acquisition phase, noise or artifact can occur in an image due to two reasons: First, the image acquisition devices induces noise/artifacts to images, as they are susceptible to thermal noise and statistical

randomness in emission of photons; second, the physiological interference, which is the inability of a patient to manage his or her physiological processes and systems. For example, the result of breathing on a chest X-ray image, movement of material through the gastrointestinal system, cardiovascular activity on CT images. It is difficult for the doctors to incur accurate and useful information from these images. The noises in the images are inevitable and hence, removing the noises is mandatory for improving the quality of the image so that the doctors can make use of these images to arrive correct conclusions. It is known that there are several physical or mechanical factors that affects these scanning devices, the researchers have to deal with different types of noises such as Rician, Gaussian, salt and pepper, shot, speckle and poisson. Each noise has its own pattern and have to be dealt with special algorithms accordingly.

From the data management point of view, digital medical images pose a great challenge as they produce extremely large data files. At the same time, existing technologies of data storage in healthcare organizations limits their efforts to cope up with huge volume of medical data. As the cloud computing provides good solutions for data storing, sharing, accessing and archiving medical imaging data, healthcare organizations are now considering cloud computing as an attractive option for managing and sharing data. Medical data sharing is always essential for these organizations, as their employees need to work together across locations and departmental boundaries. So the data needs to be transmitted across the globe for the complete integration of the employees or organizations. In addition to the occurrence of the noise in the acquisition phase, different types of noises such as additive noise, multiplicative noise and thermal noise are also introduced to the data in the transmission phase.

In this modern era, many ensemble learning techniques [5] are used to automatically detect a particular disease. These techniques need large databases as training set to learn about the disease. The learning is effective, if the training set has less noise. As the training set is not guaranteed to be noise free, various denoising techniques depending upon the applications are employed to suppress the unwanted data. The different types of noises discussed in this paper are as follows:

Random noises are caused due to the interference from random process such as thermal noise and counting of photons. The central value theorem states that irrespective of shapes of the individual random distributions, the convolution of these random functions in cascade will tend to a Gaussian distribution function. So the Gaussian noise is simulated for studying the effects of random noise and this is an additive model. Let $I_{m,n}$ be the NxN image pixels and $\eta_{m,n}$ be the NxN noise pixels where $1 \leq m,n \leq N$;

$$f_{m,n} = I_{m,n} + \eta_{m,n} \quad (1)$$

The probability density function P of a Gaussian random variable z with σ_x^2 as the variance and μ_x as the mean of the noise is given by:

$$P_x(x) = \frac{1}{\sqrt{2\pi}\sigma_x} e^{-\frac{(x-\mu_x)^2}{2\sigma_x^2}} \quad (2)$$

During transmission, the additive noise is caused due to passing automobiles, static electricity, power lines, etc., near the transmission lines. Additive White Guassian noise (AWGN) is generated from additive guassian noise. João M. Sanches, Jacinto C.

Nascimento, and Jorge S. Marques [6] removes the Guassian noise in an image by solving computationally intensive equations using numerical methods.

Noises in MR images are generally modeled as white and Rician distributed [7,8]. For the images with high SNR, Rician noise is well approximated to Guassian noise. But in low SNR cases, the Rician noise distribution is considerally different than Guassian noise. The probability of image pixels to be Rician distributed is given by

$$P_N(N) = \frac{N}{\sigma^2} e^{-\frac{I^2+N^2}{2\sigma^2}} \; E_0\left(\frac{I \,.\, N}{\sigma^2}\right) \tag{3}$$

Where N is Rician noise pixel, I is the original image and σ is the variance.

Jan Aelterman et al. [9] proposes a two-step Rician noise removal process. First, the bias is removed and then the denoising is done on the square root of the image in wavelet domain.

The uncertain behavior in the emission of photons by the sensors of the scanners leads to the poisson noise and it is characterized by a random variable represented by poisson probability distribution function. This is associated with the systems such as PET, SPECT, and fluorescent confocal microscopy imaging. Shot noise in the scanning devices can also be modeled as poisson noise. The likelihood of getting poisson noise pixel η an observed image I with λ as proportionality factor is given by:

$$\mathrm{P}(\eta_{\mathrm{m,n}} \mid \mathrm{I}_{\mathrm{m,n}}, \lambda) \; = \prod_{m,n=1}^{N} \frac{\left(\lambda \mathrm{I}_{\mathrm{m,n}}\right)^{\eta_{\mathrm{m,n}}} e^{-\lambda \mathrm{I}_{\mathrm{m,n}}}}{\eta_{\mathrm{m,n}}!} \tag{4}$$

Speckle noises occur due to the random disturbance in the coherent properties of the emitted wave in the imaging systems such as laser, acoustics and synthetic aperture radar imagery. It follows a multiplicative noise model and it estimated by generalized gamma distribution. It is represented as

$$f_{m,n} = \mathrm{I}_{\mathrm{m,n}} * \eta_{\mathrm{m,n}} \tag{5}$$

A generalized gamma random variable X with scale parameter α, and shape parameters β, and γ, gamma function Γ has probability density function:

$$P(x) = \frac{\gamma x^{\gamma\beta-1} e^{-\left(\frac{x}{\alpha}\right)^{\gamma}}}{\alpha^{\gamma\beta}\Gamma(\beta)} \tag{6}$$

During transmission, the multiplicative noise is caused due to turbulence in air, reflections, refractions, etc., on the transmission lines. Y. Guo et al. [10] modifies non-local mean filter which works better for Gaussian denoising, to adapt with the speckle reduction process. This new filter is proved to be with good denoising property along with the better edge information preservation.

Salt and pepper noises are induced due to malfunctioning of acquiring sensors and synchronization errors in transmission. It causes a sudden change in the pixel value of an image and is an impulse type of noise. Nawazish Naveeda et al. [11] used the neural

networks to detect the impulse noise and weighted average of three filters to clear out the noise in corrupted mammographic images.

In this paper, medical image denoising is done using 2-dimensional non-subsampled contourlets, curvelets and double density dual tree complex transform. The issues such as shift invariance, aliasing and lack of directionalty of the traditional Discrete Wavelet Transform (DWT) makes it ineffective in the field of medical image denoising. Over years, many variant of wavelet transforms like the double density DWT [12], dual tree complex DWT [13] are developed to overcome these disadvantages. There are many identical factors between the double density DWT and dual tree complex DWT such as shift invariance, over completeness by a factor of 2 and they both use perfectly reconstruction filter banks. The double density DWT has a single scaling function, and its output wavelets are smooth and are shift invariant. Scientists believe that the best waveform for image processing is of gabor atom which is complex in nature. To incorporate the complex nature for wavelets, a new type of wavelet called double density dual tree complex wavelet transform (DD-DTCWT) [14] combined with properties of double density DWT and dual tree complex DWT is introduced.

Curvelet [15] is a multiscale transform that efficiently represents singularities and the edges of curves. Their representation of edges are scattered than in wavelets i.e. the energy of the object is localized in few coefficients. This property of the sparseness allows for the better image reconstructions or coding algorithms.

Contourlet is the expansion of wavelet theory with the directionality and non-shift invariant property. Non-subsampled contourlet (NSCT) [16] is a directional multiresolution transform which is known for its property of shift invariance, multiscale and the preservation of vital information in natural scenes.

In this paper, the effect of different 2D geometric multiscale transforms like non-subsampled contourlets, curvelets and double density dual tree complex transform on many types of noises like AWGN, salt and pepper noise, speckle noise, and poisson noise present on MR images are analysed.

2. MATERIALS AND METHODS

2.1 Dataset

For this survey, several images from three different datasets are chosen. First subset: 100 3T brain T1 MR images are selected from MR image database provided by CASI Lab [17]. Images of patients with the history of diabetes, hypertension, head trauma, psychiatric disease, or other symptoms or history likely to affect the brain are excluded for this study. Second subset: 70 breast T1 MR images are taken from the database of The Cancer Imaging Archive (TCIA) [18]. Here, images of patients with no tumours or abnormalities are selected. Third subset: 30 heart T1 MR images are taken from cardiac MR image dataset provided by Alexander Andreopoulos and John K. Tsotsos [19,20] for research purposes.

2.2 Curvelet Transform

Curvelet transform [15] well represents the objects, shapes with smoothness except for discontinuity along a general curve with bounded curvature. It splits the frequency plane into

dyadic coronae and subdivides further into angular wedges. So it works at specified scales, locations and orientations.

Let us consider a continuous curvelet transform [21] $f \rightarrow \Gamma f(a, b, \theta)$ of functions $f(x_1, x_2)$ on R^2, with parameter space indexed by scale $a > 0$, location $b \in R^2$, and orientation θ. The coefficient are given by $\Gamma f(a, b, \theta) = \langle f, \gamma ab\theta \rangle$; the corresponding curvelet $\gamma ab\theta$ is defined by parabolic dilation in polar frequency domain coordinates. To create curvelet frame [15], the wedges are obtained by frequency tiling to find a set of curvelet functions for the frequency domain. Curvelet elements being locally supported near wedges, where the number of wedges is $N_j = 4, 2^{\lceil j/2 \rceil}$ at scale 2^{-j}. The coefficients are obtained from the functions that support the admissibility criteria [15]. Fig. 1 shows stages of denoising an image using curvelets.

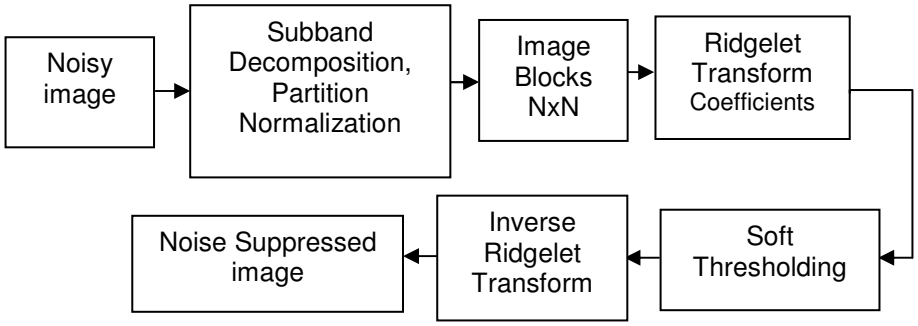

Fig. 1. Noise suppression by Curvelet Transform

H. S. Bhadauria and M. L. Dewal [22] proposed a noise suppression method by using total variation and curvelet transform method with fusion of images and is tested on CT and brain MRI images. S. Ali Hyder and R. Sukanesh [23] compares the result of the curvelet transform with different types of noises and proved that the curvelet reconstruction gives better edge preservation than wavelets.

2.3 Double Density Dual Tree Complex Wavelet Transform (DD-DTCWT)

The double density model and the dual tree DWT are mixed to create DD-DTCWTs [14]. The dual-tree DWT is a complex-valued wavelet transform which is useful for signal modeling and denoising and can be used to implement two-dimensional transforms with directional wavelets. Kingsbury's [13] idea of joining of two wavelets into Hilbert transform pairs has many advantages like near shift invariance, good denoising property, implementation of directional 2D DWTs at the same time. The oversampled filter banks also leads to good wavelet smoothness, better time frequency bandwidth and closer spacing between two wavelets of closer scale. The DD-DTCWT uses a mixture of two oversampled DWTs with oversampled iterated filter banks. The oversampled iterated filter banks of The DD-DTCWT are placed in parallel are as shown in Fig. 2.

The Hilbert transform pairs of wavelets designed to be in off-set from one another by one half, is combined with the above dual tree complex wavelet to produce DD-DTCWTs. Here, different iterated bank filters are used in both the DWTs. Fig. 3. depicts the stages of denoising an image using DD-DTCWT.

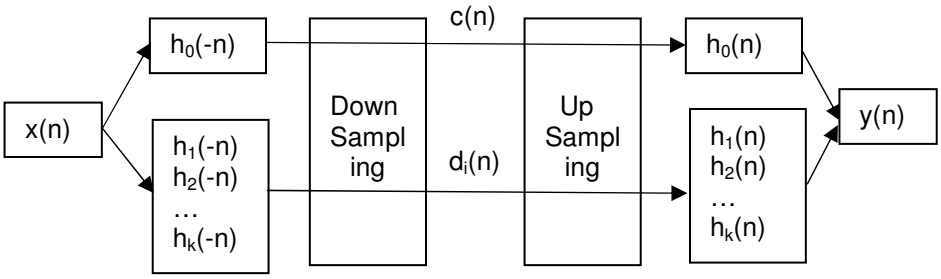

Fig. 2. Oversampled iterated filter banks

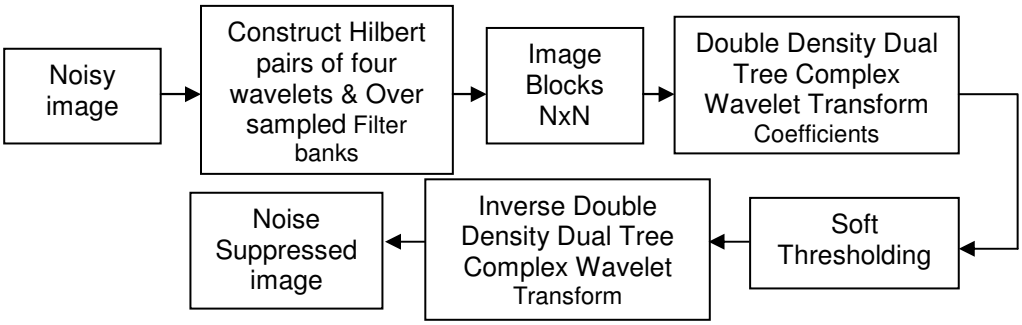

Fig. 3. Noise suppression by Double Density Dual Tree Complex Wavelet Transform

Let 2-D Dual Tree Complex Wavelet [24] be $\psi(m,n) = \psi(m)\psi(n)$ where $\psi(m)$ is a complex wavelet of form $\psi(m) = \psi_g(m) + j\psi_h(m)$.the expression $\psi(m,n)$ is given by:

$$\begin{aligned}\psi(m,n) &= \left[\psi_g(m) + j\psi_h(m)\right]\left[\psi_g(n) + j\psi_h(n)\right] \\ &= \left[\psi_g(m)\psi_g(n) + \psi_h(m)\psi_h(n)\right] + \\ &\quad j\left[\psi_g(m)\psi_h(n) + \psi_h(m)\psi_g(n)\right] \qquad (7)\end{aligned}$$

V. Naga Prudhvi Raj and T. Venkateswarlu [25] uses the shrinkage operation to remove noises from images and experiments with adding semi-soft and stein thresholding operators along with conventional hard and soft threshhold operators and proves the adaptability of dual tree complex wavelet transform in denoising medical images. Chen Bo et al. [26] combines the high directional sensitivity ridgelets and shift invariant dual tree wavelets are to denoise images. This modified ridgelet algothm is compared with weiner2 filtering and classical ridgelet image denoising. Ufuk Bal [27], uses dual tree complex wavelet transform to remove poisson noises from optical microscopy images and the analyse the results with image quality metrics.

2.4 Non-subsampled Contourlet Transform (NSCT)

This is a fully shift invariant multiscale directional transform, obtained by the frequency partitioning of wavelets that have periodically time-varying units of downsamplers and upsamplers. It is a combination of non-subsampled laplacian pyramid and directional

filterbanks (DFB) [16]. The image is divided several lowpass and highpass subbands. The lowpass and highpass directional filters are applied to the image at multiple scales. The inverse transform reconstructs the image perfectly. Fig. 4 shows the three stage pyramid reconstruction.

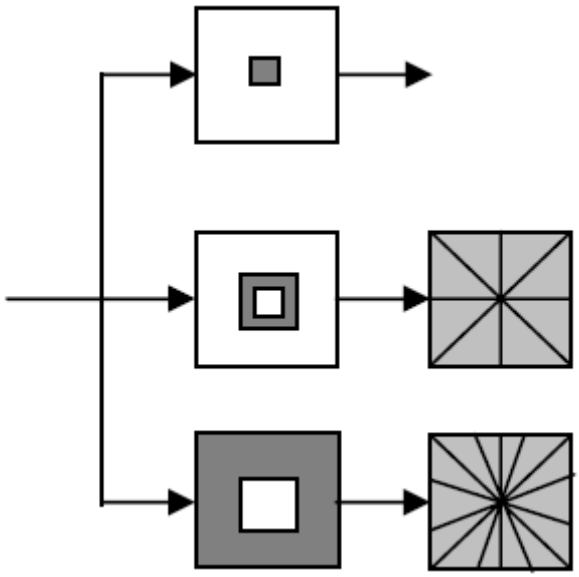

Fig. 4. Multi stage pyramid reconstruction [16]

Laplacian pyramid achieves the multiscale decomposition for the transform. Non subsampled directional filterbanks are obtained by critical oversampling of DFB of the contourlets. Fig. 5 shows various stages of denoising an image using NSCT.

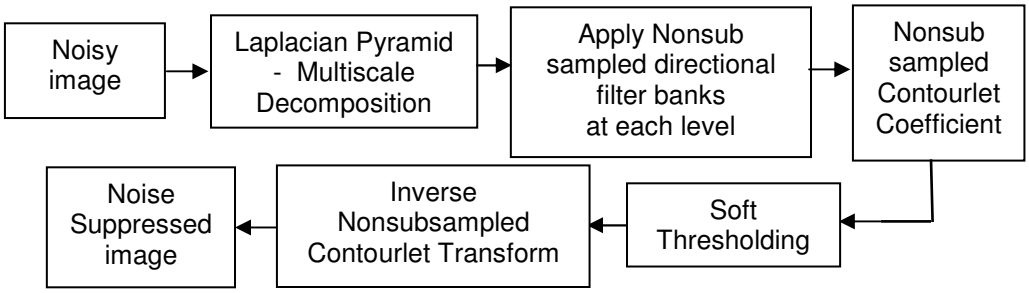

Fig. 5. Noise suppression by Nonsubsampled Contourlet Transform

Md. Foisal Hossain et al. [28] applies the least mean square error estimation on NSCT coefficients. The results show that the NSCT smooths the contour and preserves the dominant feature of the image and performs better than wavelets.

2.5 Soft Thresholding

In multiscale transformations, the thresholding can be applied at various levels of resolutions. It is proved that employing adaptive thresholding [29] at different levels of the

transform yield better results in denoising an image. Each and every subband are soft thresholded by the values calculated by taking the median values of the coefficients of the largest coefficient spectrum L_1. Noise variance is given by

$$\sigma_{L_1}^2 = \left[\frac{median(|Y_{ij}\epsilon\, L_1|)}{0.67452}\right]^2 \quad (8)$$

Threshold value is given by $\lambda_T = \frac{\sigma_{L_1}^2}{\sigma_{X_i}}$ (9)

where $\sigma_{X_i} = \sqrt{\max(\sigma_{Y_i}^2 - \sigma_{L_1}^2, 0)}$ and $\sigma_{Y_i}^2$ is the variance of the subband coefficients at i[th] level.

The scaling factor 0.67452 is best suited for the approximate estimation of Gaussian White noise [30]. The scaling factors for other types of noises like salt & pepper noise, poisson noise, speckle noise are chosen according to the performance metrics discussed in next section.

3. RESULTS AND DISCUSSION

The purpose of this paper is to analyze the performance of the 2-Dimensional multiscale transformations like nonsubsampled contourlets, curvelets, double density dual tree complex wavelets on noisy MR images. A collection of 200 MR images of brain (3T MRI scan), heart and breast are selected and input set is created by inducing the different types of noises like AWGN, Rician noise, salt and pepper noise, speckle noise and poisson noise for each image. The images are tested on the system with intel i5 processor, 4GB RAM and graphs are plotted using MATLAB R2013 software.

Image quality metrics like Peak Signal to Noise Ratio (PSNR), Mean Absolute Error (MAE), Root Mean Square Error RMSE) and Structured Similarity Index (SSIM) are calculated for assessing the performance of NSCT, Curvelet and DD-DTCWT. PSNR is the commonly used parameter for testing the quality of the reconstructed image. PSNR is more vulnerable to noises and SSIM works as the indicator that is consistent with the human eye vision model. Here, PSNR value indicates whether the reconstructed image is closer to the original image or not. More the PSNR value, better the image is restored to its original version. MAE and RMSE represent the closeness of the estimated value and the true value. Less the MAE/RMSE, more closer they are. IN CT/MR images, the structural information that holds the relationship between the objects are important, as they hold the key to earlier disease diagnosis. To effectively represent the structural dependencies of the denoised image and the original image, a metric called Structural Similarity Index (SSIM) is used. More the SSIM is close to one, more the two images are closer to each other.

The values and the graphs that are furnished below are obtained from inducing different types of noises to a 3T MRI brain scan image and calculating several quality metrics of the denoised image.

3.1 Analysis of AWGN Removal in MR Images Using NSCT, Curvelet and DD-DTCWT

For AWGN reduction analysis, noisy images of different SNR per sample are created and denoised. Different plots given in Figs. 6(a-d) shows the performance of AWGN removal

using NSCT, Curvelet, and DD-DTCWT. It is evident that NSCT woks better than Curvelet and DD-DWT. It has more PSNR, less RMSE and MAE and better SSIM. Fig. 7(a) shows brain MR image with additive noise of 10 SNR/sample and Figs. 7(b-d) shows the deonoised images using NSCT, Curvelet and DD-DTCWT. NSCT [31] have two distinct characteristics: high level of redundancy and anisotrphic contourlet basis. The high level of redundancy indicates that the NSCT coefficients of relevant data in the image present a sparse distribution in finer scale and estimation of the threshold at the finer scale gives NSCT a good noise suppressing ability. As the threshold is obtained at each finer scale, the overall average value is also used to remove additive noise model like AWGN. NSCT uses anisotrophic contourlet basis functions captures details at multiple directions and scales. The combination of these two properties makes NSCT outperforms other transforms. Paul Bao et al. [32] proposes a wavelet-based multiscale products thresholding scheme for noise suppression of MR images. First, the Multi-scale edge detection using dyadic wavelet transform is applied to noisy MR images. This wavelet transform is designed to improve the signal's instantaneous features. For the sake of fast numerical computation, the dyadic sequence is limited to 2^j. The wavelet is a quadratic spline that can be approximated to the first derivative of Guassian, which is more suitable to remove additive noise. The adjacent wavelet subbands are multiplied to improve the significant features of the images and the adaptive thresholding is done on multiscale products to give better noise removal. The perfromance of this method is measured on MSR and CNR indices on the Desired Region of Interest (DROI).

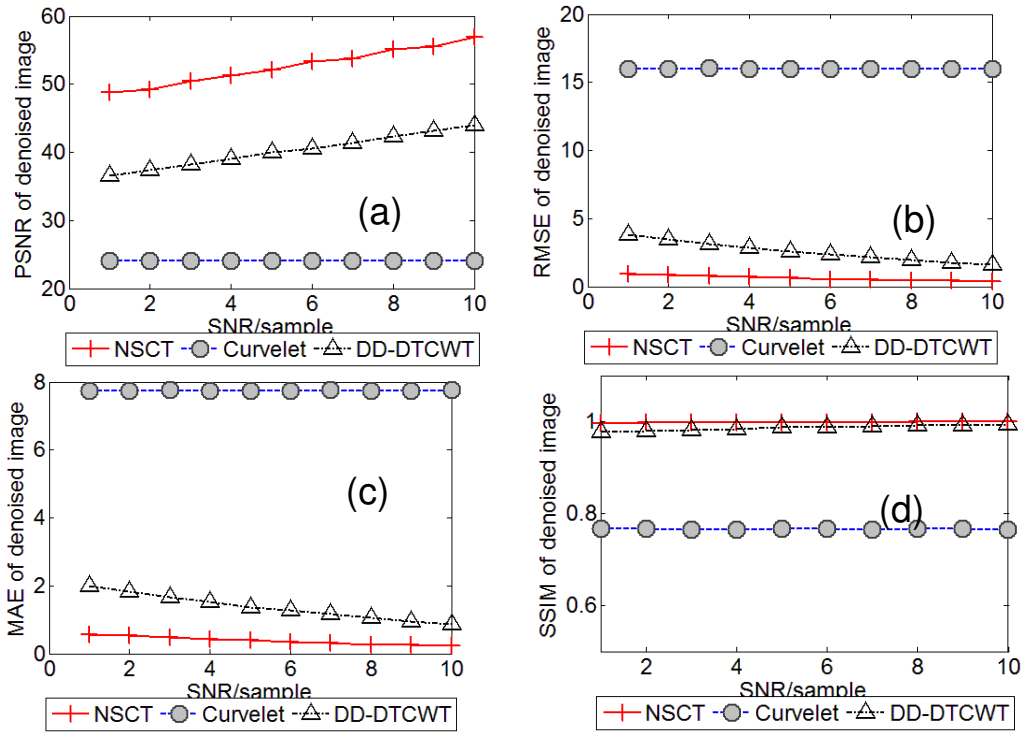

Fig. 6. (a-d) shows PSNR, RMSE, MAE & SSIM estimation of denoised 3T MRI brain scan image (AWGN) respectively

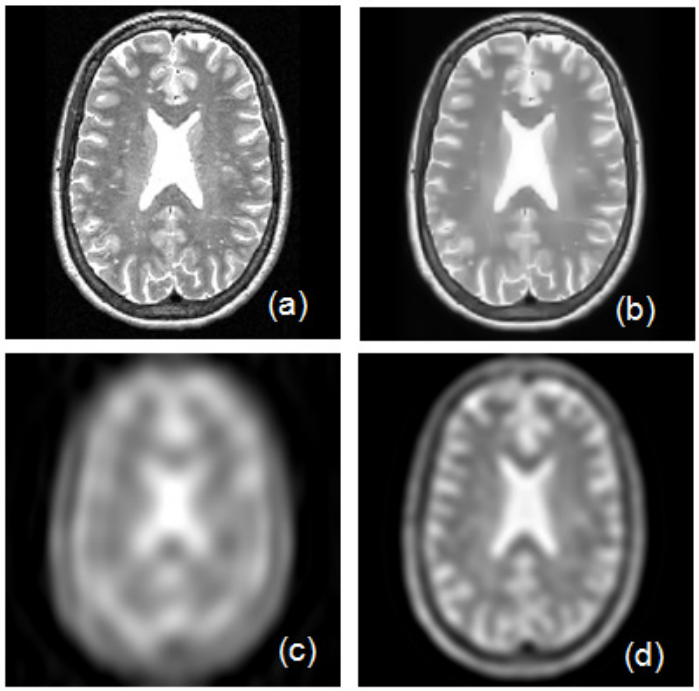

Fig. 7. (a) shows Brain MRI with AWGN(SNR/sample = 10). Fig. 7(b, c, d) shows the denoised output of NSCT, Curvelet and DD-DTCWT respectively

Florian Luisier et al. [33] uses an unbiased risk estimation procedure, to denoise the magnitude MR denoising, where the squared value of each pixel comprises an independent noncentral chi-square variate on two degrees of freedom.

3.2 Analysis of Rician Noise Removal in MR Images using NSCT, Curvelet, DD-DTCWT

For Rician noise reduction analysis, images with different Rician noise levels are created and denoised. Figs. 8(a-d) shows various performance metrics of Rician noise removal using NSCT, Curvelet, and DD-DTCWT are shown. DD-DTCWT outperforms all the other transforms. Fig. 9(a) shows breast MR image with Rician noise Variance = 0.1 and Figs. 9(b- d) shows the deonoised images using NSCT, Curvelet and DD-DTCWT.Rajeesh et al. [34] improves the quality of MR image affected with Rician noise using wave atom transform. Wave atoms accurately represents the oscillatory patterns in images. Like other transformations like wavelet or curvelet, it obeys the scaling law and retains the isotrophic aspect ratio property. These wave atoms shows sharp frequency localization that are not found in filter banks based wavelets. In this method, the noise variance are automatically computed from histogram bins of the wave atom transformed image and it is used to denoise the MR image. The result show that it performs well than wavelet shrinkage and old threshold model.

Geetika Dua et al. [35] proposes a new shrinkage threshold technique to fix the denoise threshold. Noise variance is calculated depending on the wave atom transform of the image. This method is tested on both real time and simulated images and the results shows better

performance than wavelets. Aja-Fernandez et al. [36] develops least minimum mean square error (LMMSE) for the Rician noise distribution function. The dynamic estimation of noise power is done using use the information of the sample distribution of local statistics of the image, such as the local variance, the local mean, and the local mean square value. The results show that the LMMSE estimation technique shows good performance in both noise cleaning and feature preservation. These above two methods uses multi scale transformations and gives good performance when compared with our methods.

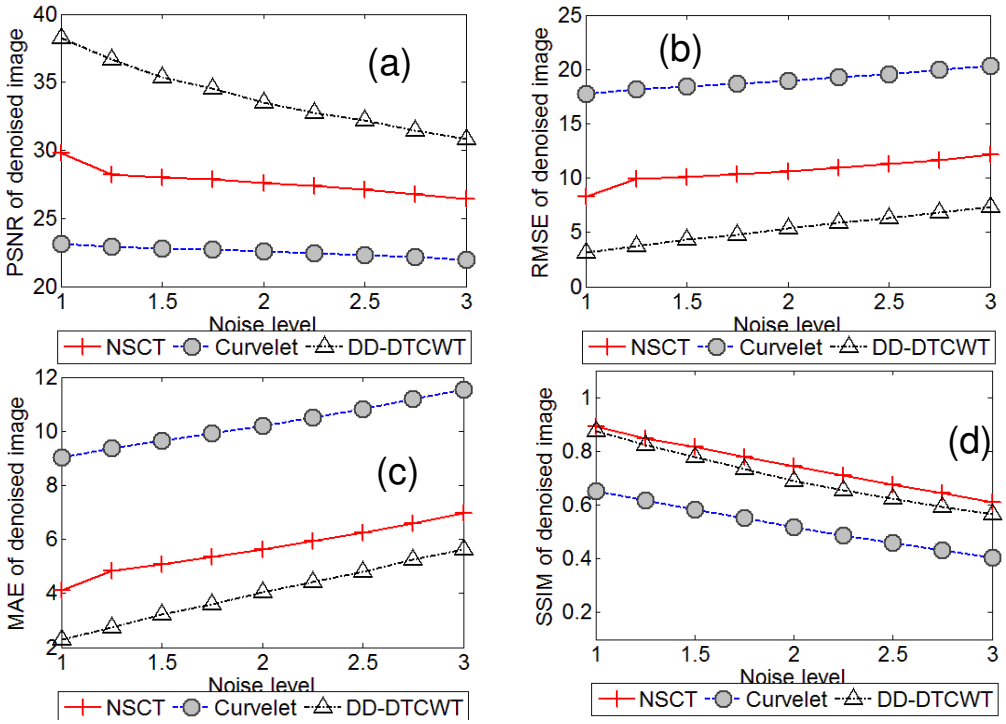

Fig. 8. (a-d) shows PSNR, RMSE, MAE and SSIM estimation of denoised 3T MRI brain scan image (Rician Noise) respectively

3.3 Analysis of Salt & Pepper Noise Removal in MR images using NSCT, Curvelet and DD-DTCWT

For Salt and Pepper Noise reduction analysis, corrupt images with different percentage of noise pixels are created and denoised. The plots of Salt and Pepper Noise removal using NSCT, Curvelet, and DD-DTCWT are shown in Figs. 10(a-d). NSCT has shown good overall image metrics. By inspecting the graphs in Fig. 10(a) and Fig. 10(b), it is inferred that, the values of the image metrics of salt and pepper noise reduction is smaller than those of the AWGN. These transforms with soft thresholding removes the random noise better than the impulse noises. The smoothness of non subsampled iterated filter banks and the multiscale decomposition makes NSCT a good transform for dealing the random and impulse noises. Raymond H. Chan et al. [37] devises a two stage process for salt and pepper noise removal. First, the pixels which have the highest probability of noise are identified by decision based median filters and then edge preserving regularization estimator is used to improve the pixels. The results show good performance even when the image is affected with 90% noise.

Ning Chun-Yu et al. [38] compares the traditional median filters and adaptive median filters in the field of denoising MR and CT images. Both filtering techniques are tested in virtual endoscope system and the adaptive median filters gives better PSNR values. The above both techniques does not use any multi-scale transformations.

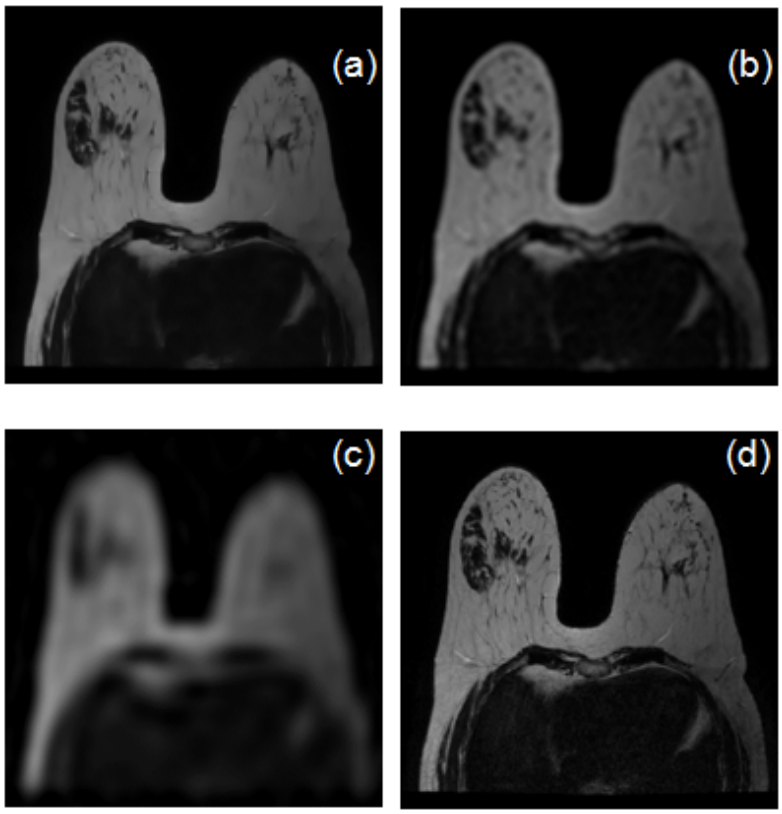

Fig. 9. (a) Shows Breast MRI with Rician noise (Variance = 0.1). Fig. 9(b-d) shows the denoised output of NSCT, Curvelet and DD-DTCWT respectively.

3.4 Analysis of Poisson Noise Removal in MR images using NSCT, Curvelet and DD-DTCWT

For Poisson noise reduction analysis, the noise with factor λ=0.5 is induced into the images and denoised. Table 1 shows the metrics of Poisson Noise removal using NSCT, Curvelet, and DD-DTCWT. It is clear that NSCT and DD-DTCWT gives better quality of reconstructed images.

Table 1. Calculated values of PSNR, RMSE, MAE and SSIM Poisson Noise Removal in MR Images using NSCT, Curvelet, and DD-DTCWT

	PSNR	RMSE	MAE	SSIM
NSCT	33.50	5.38	2.43	0.97
Curvelet	24.04	16.01	7.74	0.76
DD-DTCWT	33.36	5.47	2.70	0.96

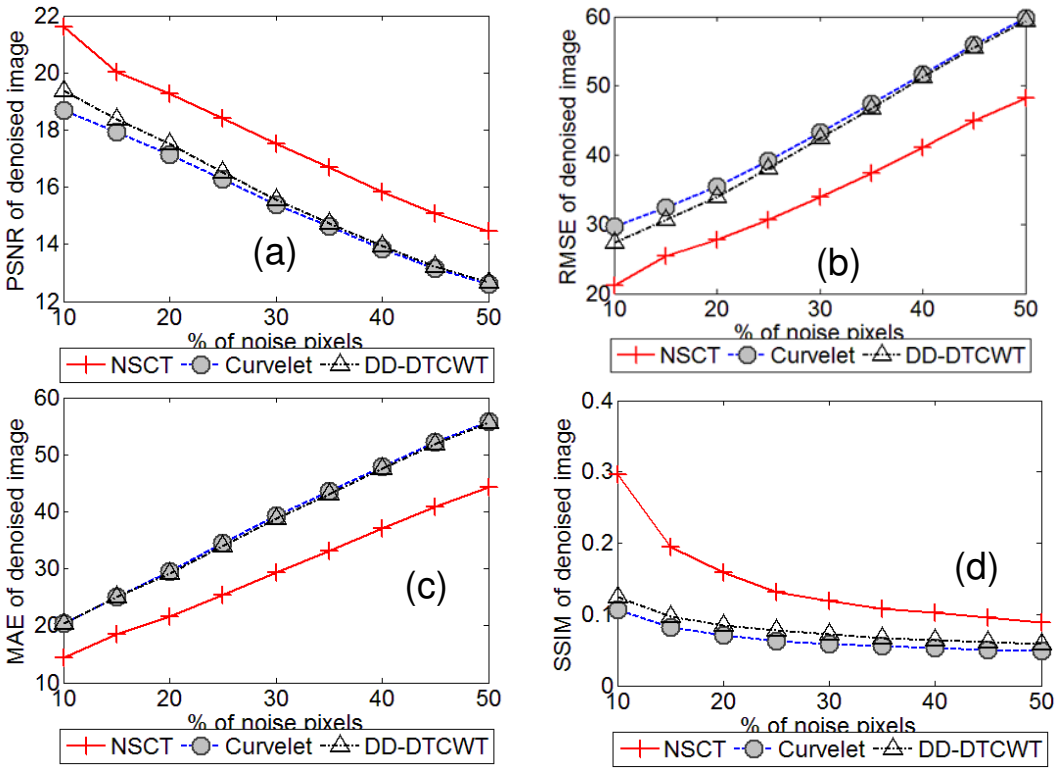

Fig. 10. (a, b, c, d) shows PSNR, RMSE, MAE & SSIM estimation of denoised 3T MRI brain scan image (Salt & Pepper Noise) respectively.

3.5 Analysis of Speckle Noise Removal in MR Images using NSCT, Curvelet, DD-DTCWT

For Speckle noise reduction analysis, images with different noise variance values are created and denoised. The plots of speckle removal using NSCT, Curvelet, and DD-DTCWT are drawn in Figs. 11(a-d) for the estimation of various performance metrics. DD-DTCWT performs well with speckle noise and shows better results than NSCT. In DD-DTCWT, the offset between the Hilbert transforms pairs is one half and the thresholding is applied for both real and imaginary coefficients of wavelets. This gives the DD-DTCWT more edge than NSCT and Curvelets in denoising speckle noise images. Fig. 12(a) shows cardiovascular MR image with Speckle noise (Variance = 0.2) and 12(b-d) shows the deonoised images using NSCT, Curvelet and DD-DTCWT.

Bo Chen et al. [39] first converts the mulitiplicative noise to additive noise in the image using Fourier transform and logarithm strategy, and then a fourth order partial differentiation equation model is created to remove the speckle noise. This model involves more computation than our method.

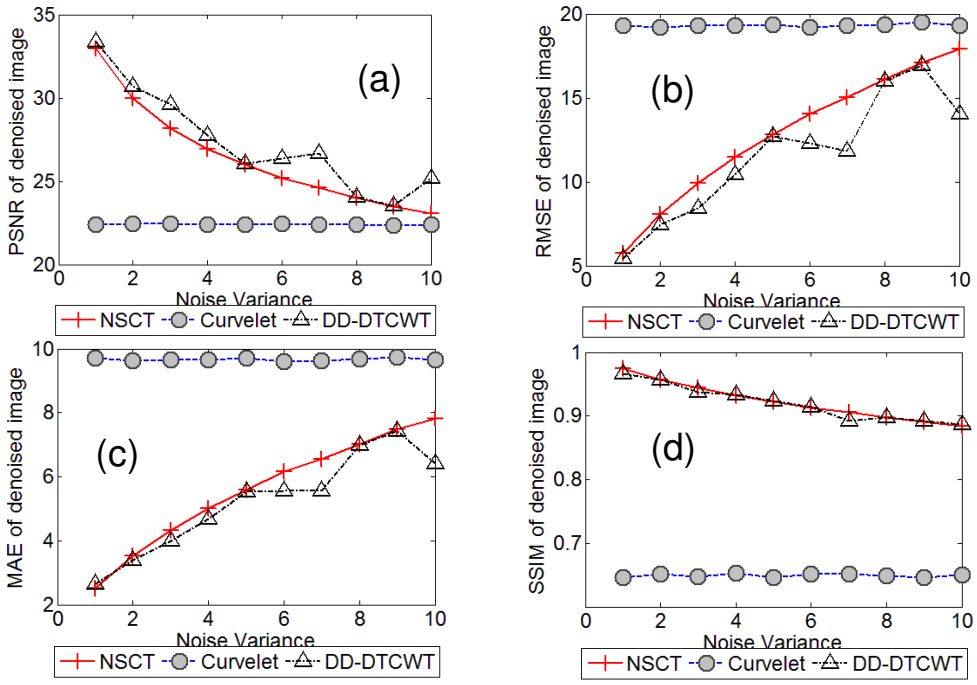

Fig. 11. (a, b, c, d) shows PSNR, RMSE, MAE & SSIM estimation of denoised 3T MRI brain scan image (Speckle Noise) respectively.

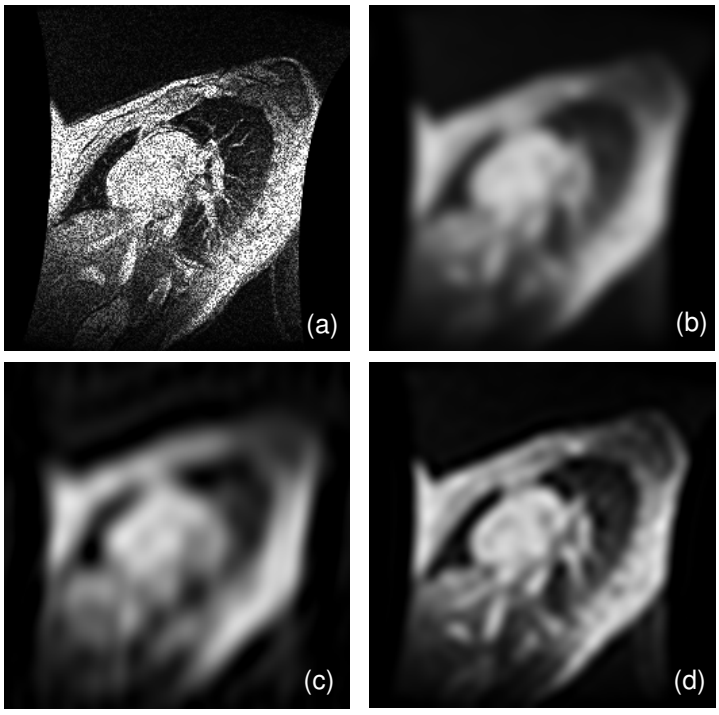

Fig. 12.(a) shows Cardiovascular MRI with Speckle noise(Variance = 0.2). Fig. 12(b, c, d) shows the denoised output of NSCT, Curvelet and DD-DTCWT respectively.

Md. Motiur Rahman et al. [40] used the median filtering technique to remove the speckle noise. The performance is measured in PSNR, Edge Preservative Factor(EPF), RMSE, Root Mean Square Error of Signal to Noise Ratio (RMSE_SNR), Ratio of gray level to preserve contrast(RM), Image Fidelity(IM) and SSIM values. Multiplicative noise removal is complex and needs algorithm with good adaptability factor.

4. CONCLUSION

In this paper, Nonsubsampled Contourlets(NSCT), Curvelets, Double Density Dual Tree Complex Wavelets(DD-DTCWT) are used to suppress noises like additive white gaussian noise, Rician noise, salt & pepper noise, poisson noise and speckle noise and the results are compared in terms of image quality metrics such as PSNR, RMSE, MAE, SSIM. For random noises and salt & pepper noises, NSCT has shown better performance metrics and produces good quality denoised biomedical images than curvelets and DD-DTCWTs. Curvelets scores poor in all the cases and its efficiency in medical image noise removal is less than other transforms. DD-DTCWT performs better than NSCT in removing speckle and Rician noises and both these transforms gives good results in removing poisson noises. Our future work will be to focus on the noise reduction analysis on MR images classification using multi-scale transformations like wavelets, shearlets, surfacelets and 3D adaptive filters.

ACKNOWLEDGEMENTS

We sincerely thank the experts of CASILab at The University of North Carolina and MIDAS Data Server at Kitware Inc., for providing the MR brain image database. We also extend our thanks to The Cancer Imaging Archive(TCIA) for breast MR images dataset and Mr. Alexander Andreopoulos amd Mr.John K. Tsotsos for the cardiac MR image dataset.

COMPETING INTERESTS

Authors have declared that no competing interests exist.

REFERENCES

1. Guorong Wua, Qian Wanga, Dinggang Shena. The Alzheimer's Disease Neuroimaging Initiative 1. Registration of longitudinal brain image sequences with implicit template and spatial–temporal heuristics. NeuroImage. 2012;59(1):404–421.
2. Pei Rui Bai, Qing Yi Liu, Lei Li, Sheng Hua Teng, Jing Li, Mao Yong Cao. A novel region-based level set method initialized with mean shift clustering for automated medical image segmentation. Computers in Biology and Medicine. 2013;43(11):1827–1832.
3. Xiaobo Qua, b, Di Guob, Bende Ninga, Yingkun Houc, Yulan Lina, Shuhui Caia, Zhong Chena. Undersampled MRI reconstruction with patch-based directional wavelets. Magnetic Resonance Imaging. 2012;30(7):964–977.
4. Seyed Morteza Hosseini, Ahmad-Reza Naghsh-Nilchi. Medical ultrasound image compression using contextual vector quantization. Computers in Biology and Medicine. 2012;42(7):743–750.

5. Manhua Liua, Daoqiang Zhanga, Dinggang Shena. The Alzheimer's Disease Neuroimaging Initiative 1. Ensemble sparse classification of Alzheimer's disease. NeuroImage. 2012;60(2):1106–1116.
6. João M. Sanches, Jacinto C. Nascimento, and Jorge S. Marques. Medical Image Noise Reduction Using the Sylvester–Lyapunov Equation. IEEE Trans. on Image Processing. 2008;17(9):1522-1539.
7. Sijbers J, den Dekker AJ, Scheunders P, Dyck DV. Maximum-likelihood estimation of Rician distribution parameters. IEEE Trans. on Medical Imaging. 1998;17:357-361.
8. Nowak R. Wavelet-based rician noise removal for magnetic resonance imaging. IEEE Trans. on Image Processing. 1999;10:1408–1419.
9. Jan Aelterman, Bart Goossens, Aleksandra Pizurica and Wilfried Philips. Removal of Correlated Rician Noise in Magnetic Resonance Imaging. 16th European Signal Processing Conference - EUSIPCO '08. 2008;25-29.
10. Guo Y, Wang Y, Hou T. Speckle filtering of ultrasonic images using a modified non local-based algorithm. Biomedical Signal Processing and Control. 2011;6(2):129–138.
11. Nawazish Naveeda, Ayyaz Hussainb, M. Arfan Jaffara, Tae-Sun Choic. Quantum and impulse noise filtering from breast mammogram images. Computer Methods and Programs in Biomedicine. 2012;108(3):1062–1069.
12. Yu-Long Qiao, Chun-Yan Song, Chun-Hui Zhao. Double-Density Discrete Wavelet Transform Based Texture Classification. Third International Conference on Intelligent Information Hiding and Multimedia Signal Processing - IIHMSP '07. 2007;1:91–94.
13. Kingsbury NG. The Dual Tree Complex Wavelet Transform. A New Technique For Shift Invariance And Directional Filters. In Proceedings of the Eighth IEEE DSP Workshop, Utah; 1998.
14. Ivan W. Selesnick. The Double-Density Dual-Tree DWT. IEEE Transactions On Signal Processing. 2004;52(5):1304-1314.
15. Jianwei Ma, Plonka, G. The Curvelet Transform. IEEE, Signal Processing Magazine. 2010;27(2):118 – 133.
16. Arthur L. da Cunha, Jianping Zhou, Minh N. Do. The Non-subsampled Contourlet Transform: Theory, Design, and Applications. IEEE Transactions on Image Processing. 2006;15(10).
17. Bullitt E, Zeng D, Gerig G, Aylward S, Joshi S, Smith JK, Lin W, Ewend MG. Vessel tortuosity and brain tumor malignancy: A blinded study. Academic Radiology. 2005:12:1232-1240.
18. Web Resource. Breast MR image dataset, The Cancer Imaging Archive (TCIA). Available: http://www.cancerimagingarchive.net/
19. Alexander Andreopoulos, John K. Tsotsos. Efficient and Generalizable Statistical Models of Shape and Appearance for Analysis of Cardiac MRI, Medical Image Analysis. 2008:12(3):335-357.
20. Web Resource. Cardiac MRI dataset. Available: http://www.cse.yorku.ca/~mridataset/
21. Emmanuel J. Candèsa, David L. Donohob. Continuous curvelet transform: II. Discretization and frames. Applied and Computational Harmonic Analysis. 2005;19(2):198–222.
22. Bhadauria HS, Dewal ML. Medical image denoising using adaptive fusion of curvelet transform and total variation. Computers & Electrical Engineering. 2013;39(5):1451–1460.

23. Ali Hyder S, Sukanesh R. An Efficient Algorithm for Denoising MR and CT Images Using Digital Curvelet Transform. Advances in Experimental Medicine and Biology. 2011;696:471-480.
24. Ivan W. Selesnick, Richard G. Baraniuk, Nick G. Kingsbury. The Dual-Tree Complex Wavelet Transform. IEEE, Signal Processing Magazine. 2005;22(6):123–151.
25. Naga Prudhvi Raj V, Venkateswarlu T. Denoising of Medical Images Using Dual Tree Complex Wavelet Transform. Procedia Technology, 2nd International Conference on Computer, Communication, Control and Information Technology. 2012;4:238–244.
26. Chen Bo, Geng Zexun, Yang Yang, Shen Tianshuang. Dual-tree Complex Wavelets Transforms for Image Denoising. 8th International Conference on Software Engineering, Artificial Intelligence, Networking, and Parallel/Distributed Computing. 2007;1:70-74.
27. Ufuk Bal, Dual tree complex wavelet transform based denoising of optical microscopy images. Biomedical Optics Express. 2012;3(12):3231-3239.
28. Md. Foisal Hossain, Mohammad Reza Alsharif, Katsumi Yamashita. LMMSE-Based Image Denoising in Non-subsampled Contourlet Transform Domain. Image and Signal Processing, Lecture Notes in Computer Science. 2010;6134:36-43.
29. Grace Chang S, Bin Yu, Martin Vetterli. Adaptive Wavelet Thresholding for Image Denoising and Compression. IEEE Transactions on Image Processing. 2009;9(9).
30. Donald B. Percival, Andrew T. Walden. Wavelet Methods for Time Series Analysis. 1st ed. Cambridge University Press; 2006.
31. Yuxin Ma, Jiancang Xie, Jungang Luo. Image Enhancement Based on Non-subsampled Contourlet Transform. Fifth International Conference on Information Assurance and Security. 2009;1:31-34.
32. Paul Bao, Lei Zhang. Noise Reduction for Magnetic Resonance Images Via Adaptive Multiscale Products Thresholding. IEEE Transactions on Medical Imaging. 2003;22(9):1089–1099.
33. Florian Luisier, Thierry Blu, Fellow, and Patrick J. Wolfe. A Cure for Noisy Magnetic Resonance Images: Chi-Square Unbiased Risk Estimation. IEEEE Transactions on Image Processing, 2012:21(8):3454 – 3466.
34. Rajeesh J., Moni R.S., Kumar S.P. Gopalakrishnan T. Rician Noise Removal on MRI Using Wave Atom Transform With Histogram Based Noise Variance Estimation. IEEE International Conference on Communication Control and Computing Technologies (ICCCCT). 2010;531-535.
35. Geetika Dua, Varun Raj, Mri Denoising Using Waveatom Shrinkage. Global Journal of Researches in Engineering, Electrical and Electronics Engineering. 2012;12(4).
36. Aja-Fernandez S, Alberola-Lopez C, Westin CF. Noise and Signal Estimation In Magnitude MRI And Rician Distributed Images: A LMMSE Approach. IEEE Transactions on Image Processing. 2008;7(8):1383–1398.
37. Raymond H. Chan, Chung-Wa Ho, Mila Nikolova. Salt-And-Pepper Noise Removal by Median-Type Noise Detectors and Detail-Preserving Regularization. IEEE Transactions on Image Processing. 2005;14(10):1479-1485.
38. Ning Chun-Yu, Liu Shu-Fen, Qu Ming. Research on Removing Noise in Medical Image Based on Median Filter Method. IEEE International Symposium on IT in Medicine & Education (ITIME). 2009;1:384-388.

39. Bo Chen, Jin-Lin Cai, Wen-Sheng Chen, Yan Li. A Multiplicative Noise Removal Approach Based on Partial Differential Equation Model. Mathematical Problems in Engineering. 2012;2012.
40. Motiur Rahman, Shohel Rana, Aminul Islam, Masudur Rahman, Mehedi Hasan Talukder. A New Filtering Technique For Denoising Speckle Noise From Medical Images Based on Adaptive and Anisotropic Diffusion Filter. 2013;2(9):685-688.

Peer-review history:
The peer review history for this paper can be accessed here:
http://www.sciencedomain.org/review-history.php?iid=529&id=32&aid=4618